SECTION 4
IDENTIFICATION OF STRUCTURAL PROPERTIES

4.1 Introduction

The identification of the properties of the structure without fluid dampers was easily accomplished by established procedures. The amplitudes of transfer functions of total acceleration under white noise excitation of lightly damped structures contain sharp and narrow peaks which reveal frequencies, damping ratios and mode shapes.

However, the transfer functions of highly damped structures do not usually contain well defined peaks and identification of the structural properties is not directly possible.

The approach followed herein for the identification of the damped structure was based on a calibrated analytical model of the structure. The analytical model was constructed from the properties of the undamped structure and with the effect of fluid dampers included. For this, the constitutive model of Section 2 was utilized. The analytical model was then verified by comparison of analytical to experimental transfer functions. The structural properties were then determined by solution of the eigenvalue problem of the damped structure.

4.2 Identification of One-story Structure

The structural properties of the one-story structure with supplemental dampers can be determined from the equation of motion

$$m\ddot{u} + c_u\dot{u} + ku + \eta P_d = -m\ddot{u}_g \qquad (4\text{-}1)$$

where m is the mass of the structure, k is the stiffness of the undamped structure, c_u is the damping constant of the structure without dampers, η is the number of dampers, P_d is the horizontal

component of force in a single damper, $\ddot{u}_g$ is the ground acceleration; and $\ddot{u}$, $\dot{u}$, and u are the relative acceleration, velocity, and displacement, respectively, of the mass. The constitutive equation of the dampers has been given previously in its most general form by Equation 2-13. For a damper inclined at an angle θ with respect to the horizontal axis, the equation in the horizontal direction becomes

$$P_d + \lambda \dot{P}_d = C_o \dot{u} \cos^2\theta \qquad (4\text{-}2)$$

The amplitude of the total acceleration transfer function or absolute transmissibility, T (Harris 1987), is defined as the ratio of the steady-state total acceleration ($\ddot{u} + \ddot{u}_g$) amplitude to the amplitude of the harmonic ground motion. It may be derived by application of Fourier transform to Equations 4-1 and 4-2:

$$T = \left| 1 + \omega^2 \left[-\omega^2 + \omega_n^2 + 2i\omega\omega_n\xi_u + \frac{i\eta\omega C_o \cos^2\theta}{m(1 + i\omega\lambda)} \right]^{-1} \right| \qquad (4\text{-}3)$$

where ω_n is the natural frequency of the structure without dampers, i is the imaginary unit, and ξ_u is the damping ratio of the undamped structure. Furthermore, in Equation 4-3, the vertical lines stand for the modulus of the contained complex quantity.

Experimental transfer functions are obtained in exactly the same manner. The structure is excited by stationary banded white noise excitation and records of the total acceleration are obtained. The transfer function is then calculated as the ratio of the Fourier amplitude of the recorded total acceleration to the Fourier amplitude of the ground acceleration.

In the case of a structure without fluid dampers, $\eta = 0$ and Equation 4-3 assumes a simple form involving the structural properties of natural frequency, ω_n, and damping ratio, ξ_u. For

lightly damped structures ($\xi_u < 0.1$), the position and magnitude of the single sharp peak in the transfer function determines the structural properties.

The eigenvalue problem of the structure with fluid dampers requires a numerical procedure. Equations 4-1 and 4-2, with $\ddot{u}_g$ set equal to zero, are written in matrix form, having first introduced a new vector $\{Z\}$:

$$\{Z\} = \lfloor \dot{u} \quad u \quad P_d \rfloor \tag{4-4}$$

$$[B]\{\dot{Z}\} + [A]\{Z\} = \{0\} \tag{4-5}$$

where

$$[B] = \begin{bmatrix} 1 & 0 & 0 \\ 0 & 1 & 0 \\ 0 & 0 & \lambda \end{bmatrix} \tag{4-6}$$

$$[A] = \begin{bmatrix} 2\xi_u\omega_n & \omega_n^2 & m^{-1} \\ -1 & 0 & 0 \\ -\eta C_o \cos^2\theta & 0 & 1 \end{bmatrix} \tag{4-7}$$

For a solution of the form

$$\{Z\} = \{Z_o\}\, e^{\mu t} \tag{4-8}$$

Equation 4-5 reduces to

$$[A]\{Z_o\} = -\mu [B]\{Z_o\} \tag{4-9}$$

Equation 4-9 describes a generalized eigenvalue problem. The solution of this problem (e.g., IMSL 1987) will result in values of the eigenvalue μ.

The frequency, ω_1, and damping ratio, ξ_1, are determined by recalling the expression for the characteristic roots of the

equation of free vibration of a viscously damped single degree of freedom system:

$$\mu = -\xi_1\omega_1 \pm i\omega_1 \ (1 - \xi_1^2)^{1/2} \tag{4-10}$$

Accordingly,

$$\omega_1 = | \mu | \tag{4-11}$$

$$\xi_1 = - \frac{\mathbf{R}(\mu)}{\omega_1} \tag{4-12}$$

where | | stands for the modulus and $\mathbf{R}$ for the real part of μ.

4.3 Identification of Multistory Structure

4.3.1 Structure without Fluid Dampers

The equations of motion of a base excited multi-degree of freedom lumped mass structure may be written in the following form

$$[M]\{\ddot{u}\} + [C_u]\{\dot{u}\} + [K]\{u\} = -[M]\{R\}\ \ddot{u}_g \tag{4-13}$$

where $[M]$ is the mass matrix, $[C_u]$ is the damping matrix, $[K]$ is the stiffness matrix; $\{\ddot{u}\}$, $\{\dot{u}\}$, and $\{u\}$ are the vectors of relative acceleration, velocity, and displacement of the degrees of freedom, respectively. Furthermore, $\{R\}$ is a vector which, for a structure with one degree of freedom per floor, contains units.

Expressing the displacement vector in terms of modal coordinates, y_k:

$$\{u\} = \sum_{k=1}^{K} \{\phi_k\}\ y_k \tag{4-14}$$

where $\{\phi_k\}$ is the k-th modal vector (or mode shape), and k is the number of degrees of freedom.

The amplitude of the transfer function of degree of freedom j may be obtained by application of Fourier transform:

$$T_j = \left| \sum_{k=1}^{K} \frac{-\Gamma_k \ (2i\omega\xi_k\omega_k + \omega_k^2)}{\omega_k^2 - \omega^2 + 2i\xi_k\omega\omega_k} \ \phi_{jk} \right| \qquad (4\text{-}15)$$

where ω_k and ξ_k are the k-th mode frequency and damping ratio, ϕ_{jk} is the component of mode shape $\{\phi_k\}$ corresponding to degree of freedom j and Γ_k is the k-th modal participation factor given by

$$\Gamma_k = \frac{-\{\phi_k\}^T \ [M] \ \{R\}}{\{\phi_k\}^T \ [M] \ \{\phi_k\}} \qquad (4\text{-}16)$$

For a lightly damped structure ($\xi_k < 0.1$), the k-th peak of the amplitude of the transfer function, T_j, occurs at frequency ω_k. Furthermore, if we assume well separated modes, the term in front of $\{\phi_{jk}\}$ in Equation 4-15 is equal to a negligible value for all frequencies $\omega \neq \omega_k$. Accordingly, Equation 4-15 simplifies to

$$T_j(\omega_k) \approx \frac{\Gamma_k \ (1 + 4\xi_k^2)}{2\xi_k} \ \phi_{jk} \qquad (4\text{-}17)$$

It should be noted that the term in front of ϕ_{jk} in Equation 4-17 is a constant. Therefore, the magnitude of the peak at frequency ω_k of function T_j is proportional to the magnitude of the k-th mode shape corresponding to the j-th degree of freedom. Thus, the position and magnitude of the peaks of experimental transfer functions of all degrees of freedom directly yield the frequencies and mode shapes. Use of Equations 4-16 and 4-17 determines the corresponding damping ratios.

4.3.2 Construction of Stiffness and Damping Matrices

The stiffness matrix, $[K]$, and the damping matrix, $[C_u]$, are constructed from the experimentally determined frequencies, damping ratios, and mode shapes using a procedure described by Clough (1975). The undamped eigenvalue equation is given by

$$\omega_k^2 [M]\{\phi_k\} = [K]\{\phi_k\} \tag{4-18}$$

where ω_k is the frequency corresponding to the k-th mode of vibration, and $\{\phi_k\}$ is the mode shape. The generalized mass and stiffness matrices are given by

$$[M^*] = [\phi]^T [M] [\phi] \tag{4-19}$$

$$[K^*] = [\phi]^T [K] [\phi] \tag{4-20}$$

where $[\phi]$ is the mode shape matrix containing the mode shapes $\{\phi_k\}$. The orthogonality of the mode shapes relative to the mass matrix can be used to obtain the following relationship

$$[\phi]^{-1} = [M^*]^{-1} [\phi]^T [M] \tag{4-21}$$

Using Equations 4-20 and 4-21, the stiffness matrix, $[K]$, can be determined as

$$[K] = [M][\phi][M^*]^{-1}[K^*][M^*]^{-1}[\phi]^T[M] \tag{4-22}$$

The matrix $[M^*]$ is diagonal with elements m_k^* given by

$$m_k^* = \{\phi_k\}^T [M] \{\phi_k\} \tag{4-23}$$

Equations 4-22 and 4-23 are combined to give

$$[K] = [M] \left(\sum_{k=1}^{K} \frac{\omega_k^2}{m_k^*} \{\phi_k\}\{\phi_k\}^T \right) [M] \tag{4-24}$$

where k is the number of modes.

In a similar way, the damping matrix is evaluated as

$$[C_u] = [M] \left(\sum_{k=1}^{K} \frac{2\xi_k \omega_k}{m_k^*} \{\phi_k\} \{\phi_k\}^T \right) [M] \qquad (4\text{-}25)$$

where ξ_k is the damping ratio corresponding to the k-th mode.

4.3.3 Equations of Motion of Structure with Fluid Dampers

The equations of motion of the structure without dampers (Equation 4-13) are augmented by the vector $\{P_d\}$ which contains the horizontal components of damper forces acting on the floors. For a structure modeled with one degree of freedom per floor, the equation of motion is

$$[M]\{\ddot{u}\} + [C_u]\{\dot{u}\} + [K]\{u\} + \{P_d\} = -[M]\{1\}\ \ddot{u}_g \qquad (4\text{-}26)$$

$$\{P_d\} = \begin{Bmatrix} \eta_N P_N \\ \vdots \\ \eta_j P_j - \eta_{j+1} P_{j+1} \\ \vdots \\ \eta_1 P_1 - \eta_2 P_2 \end{Bmatrix} \qquad (4\text{-}27)$$

where η_j is the number of dampers at the j-th story and P_j is the horizontal component of force in a damper at the j-th story. It is assumed here that all dampers at a story are identical.

The general constitutive equation describing the damper force P_j is

$$P_j + \lambda \frac{dP_j}{dt} = C_o \cos^2\theta_j \frac{d}{dt}(u_j - u_{j-1}) \qquad (4\text{-}28)$$

in which θ_j is the angle of placement of damper j with respect to the horizontal and $u_o = 0$ $(j = 1)$.

Application of Fourier transform to Equations 4-26 to 4-28 results in

$$[S(\omega)]\{\bar{u}\} = -[M]\{1\}\,\bar{\ddot{u}}_g \qquad (4\text{-}29)$$

in which the overbar denotes the Fourier transform and matrix $[S]$ represents the dynamic stiffness matrix:

$$S(\omega) = -\omega^2[M] + i\omega[C_v] + [K] + [D(\omega)] \qquad (4\text{-}30)$$

Matrix $[D]$ contains the contribution of the damper forces to the dynamic stiffness matrix.

The construction of matrix $[D]$ is given below for two of the three tested configurations which are depicted in Figure 3-3. It should be noted that all dampers are identical.

$$[D] = \frac{i\omega}{1 + i\omega\lambda}\,[C] \qquad (4\text{-}31)$$

where for the case of two dampers at the first story

$$[C] = \begin{bmatrix} 0 & 0 & 0 \\ 0 & 0 & 0 \\ 0 & 0 & C_1 \end{bmatrix} \qquad (4\text{-}32)$$

and for the case of six dampers

$$[C] = \begin{bmatrix} C_3 & -C_3 & 0 \\ -C_3 & C_2 + C_3 & -C_2 \\ 0 & -C_2 & C_1 + C_2 \end{bmatrix} \qquad (4\text{-}33)$$

In the above equations,

$$C_i = 2C_o\cos^2\theta_i \;; \qquad i = 1,\ 2 \text{ and } 3 \qquad (4\text{-}34)$$

4.3.4 Transfer Functions of Structure with Fluid Dampers

Defining the inverse of matrix $[S]$ as $[H]$, Equation 4-29 may be solved for $\{\overline{u}\}$. Upon multiplication by $-\omega^2$, the Fourier transform of the relative acceleration vector is obtained:

$$\{\overline{\ddot{u}}\} = \omega^2 [H] [M] \{1\} \overline{\ddot{u}}_g \tag{4-35}$$

The amplitude of the transfer function of the j-th degree of freedom is by definition

$$T_j = \left| \frac{\overline{\ddot{u}}_g + \overline{\ddot{u}}_j}{\overline{\ddot{u}}_g} \right| \tag{4-36}$$

or

$$T_j = \left| 1 + \omega^2 \sum_{k=1}^{K} H_{jk}(\omega)\, m_k \right| \tag{4-37}$$

where H_{jk} are elements of matrix $[H]$ and m_k is the lumped mass at the k-th floor.

4.3.5 Eigenvalue Problem of Structure with Fluid Dampers

The eigenvalue problem is formulated and solved in the same way as that of the one story structure (Section 4.2).

Vector $\{Z\}$ is defined as

$$\{Z\} = \begin{Bmatrix} \{\dot{u}\} \\ \{u\} \\ \{P_d\} \end{Bmatrix} \tag{4-38}$$

Equation 4-5 is valid with matrix $[A]$ and $[B]$ given, in the case of the tested structure, by

$$[B] = \begin{bmatrix} [M] & [0] & [0] \\ [0] & [I] & [0] \\ [0] & [0] & \lambda[I] \end{bmatrix} \tag{4-39}$$

$$[A] = \begin{bmatrix} [C_v] & [K] & [I] \\ -[I] & [0] & [0] \\ -[C] & [0] & [I] \end{bmatrix} \tag{4-40}$$

where $[I]$ is the identity matrix.

It should be noted that the solution of Equation 4-5 will result in the eigenvectors $\{Z_o\}$, a portion of which contains the complex-valued mode shapes.

4.4 Identification Tests

Identification tests were conducted by exciting the base of the model structure with a banded, 0 to 20 Hz white noise of peak acceleration equal to 0.05g. In the case of the structures without fluid dampers, the structural properties were identified by the procedure of Section 4.3. In the case of the structures with fluid dampers, the properties were analytically determined using the procedures of Sections 4.2 and 4.3 and utilizing the identified properties of the bare frame and the calibrated model of the fluid dampers (at room temperature).

The properties are presented in Tables 4-I and 4-II. In the case of the one-story structure, Table 4-I includes properties identified in the seismic tests. Recorded base shear - drift loops were used to obtain the stiffness, energy dissipated in a full cycle, W_d, and elastic energy stored at maximum drift, W_s. The damping was then calculated according to Clough (1975):

TABLE 4-I Properties of One-Story Model Structure

UNSTIFFENED STRUCTURE	0 DAMPERS Small Amplitude Vibration	0 DAMPERS Seismic Motion	2 DAMPERS	4 DAMPERS
Frequency (Hz)	2.00	1.94	2.04	2.10
Damping Ratio (%)	0.55	2.2	28.4	57.7

STIFFENED STRUCTURE	0 DAMPERS Small Amplitude Vibration	0 DAMPERS Seismic Motion	2 DAMPERS	4 DAMPERS
Frequency (Hz)	3.13	2.99	3.27	3.35
Damping Ratio (%)	2.0	2.9	19.3	37.4

STIFFENED STRUCTURE WITH CABLES	0 DAMPERS Small Amplitude Vibration	0 DAMPERS Seismic Motion	2 DAMPERS	4 DAMPERS
Frequency (Hz)	---	3.17	---	---
Damping Ratio (%)	---	5.1	---	---

TABLE 4-II Properties of 3-story Model Structure at Small Amplitude of Vibration

		0 DAMPERS			2 DAMPERS			4 DAMPERS			6 DAMPERS		
	MODE	1	2	3	1	2	3	1	2	3	1	2	3
Frequency (Hz)		2.00	6.60	12.20	2.03	6.88	12.34	2.11	7.52	12.16	2.03	7.64	16.99
Damping Ratio (%)		1.74	0.76	0.34	9.90	14.72	5.02	17.7	31.85	11.33	19.40	44.70	38.04
Mode Shape	Floor 1	0.417	-1.306	1.810									
	Floor 2	0.765	-0.595	-2.293									
	Floor 3	1.000	1.000	1.000									

$$\xi = \frac{W_d}{4\pi W_s} \qquad (4\text{-}41)$$

while the frequency was calculated from the measured stiffness and known mass.

The results in Tables 4-I and 4-II demonstrate the following:

a) The structure without fluid dampers exhibits, under seismic motion, damping in the range of 2 to 5 percent of critical. This shows that the structure was realistically damped.

b) The fluid dampers had a primary effect of increasing damping. The effect on the fundamental frequency is, as expected, small and amounts to an increase of stiffness of generally less than 10 percent.

c) The effect of fluid dampers on the higher mode frequencies is important. This was expected since these frequencies are above 4 Hz, the range in which the dampers develop significant stiffness.

d) The addition of fluid dampers in only the first story of the 3-story model resulted in significant modification of the modal damping properties. This interesting observation will be further discussed in Sections 5 and 6.

e) The one-story structure in its stiffened configuration without dampers experienced some inelastic action during seismic testing. This is evident in its reduction of frequency and increase in damping in comparison to tests at small amplitude vibration. If one assumes elastoplastic behavior, the observed reduction of frequency corresponds to a displacement ductility of about 1.2.

The accuracy of the analytical model of Sections 4.2 and 4.3 is demonstrated in Figures 4-1 to 4-3, which compare analytical and experimental amplitudes of transfer functions. The comparison is

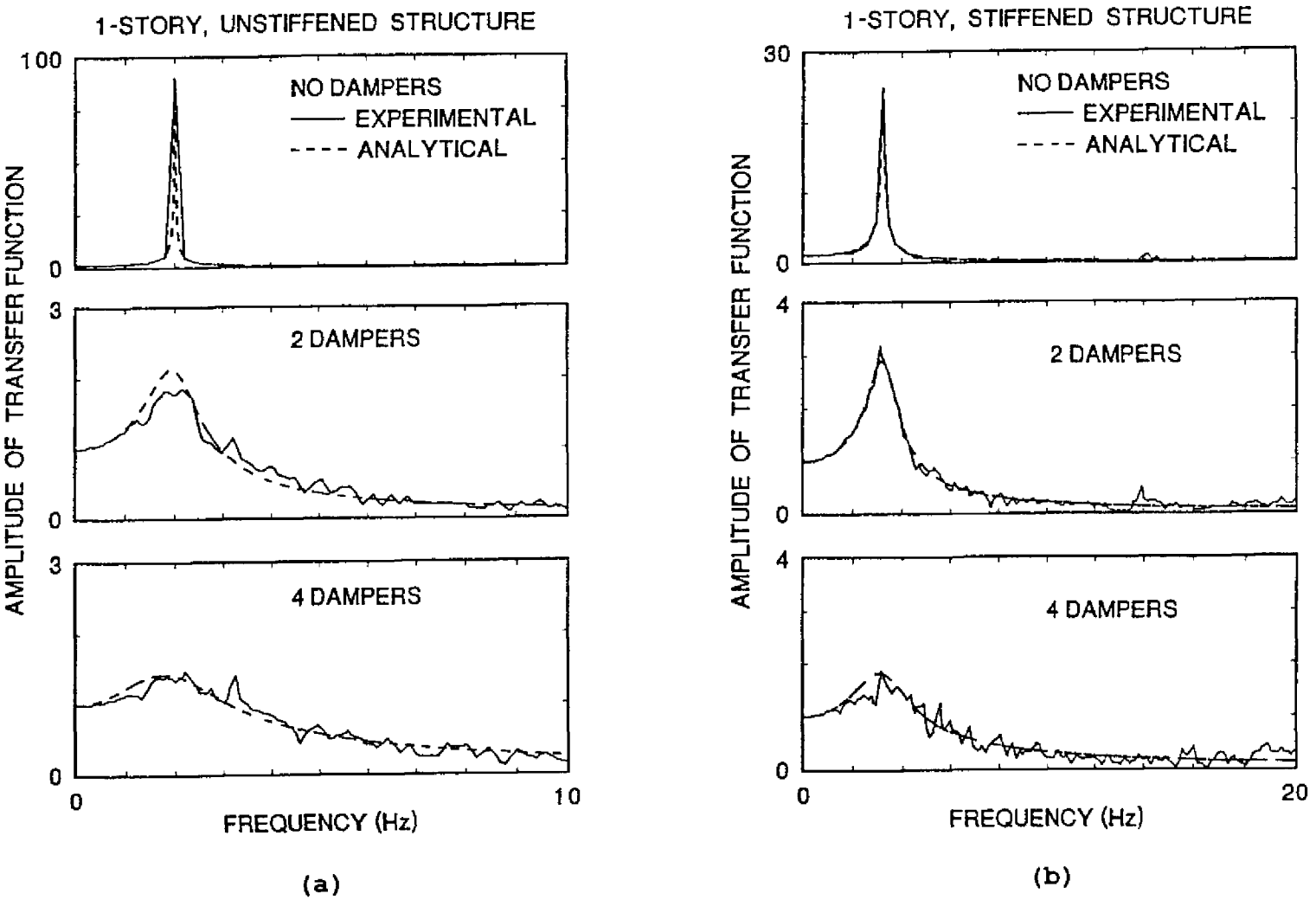

FIGURE 4-1 Comparison of Analytical and Experimental Amplitudes of Transfer Functions of One-story (a) Unstiffened Structure and (b) Stiffened Structure

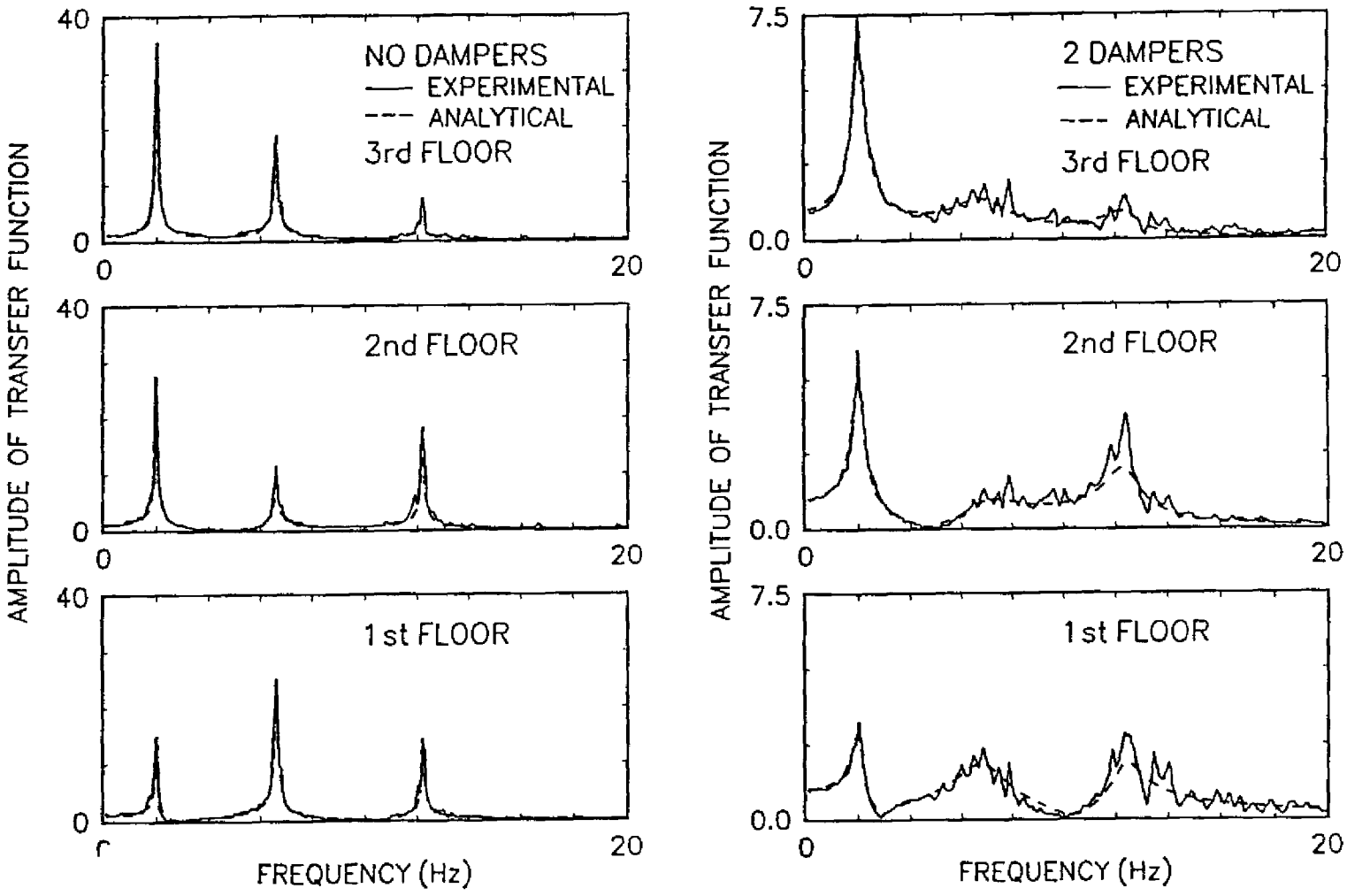

FIGURE 4-2 Comparison of Analytical and Experimental Amplitudes of Transfer Functions of 3-story Structure with (a) No Dampers and (b) Two Dampers

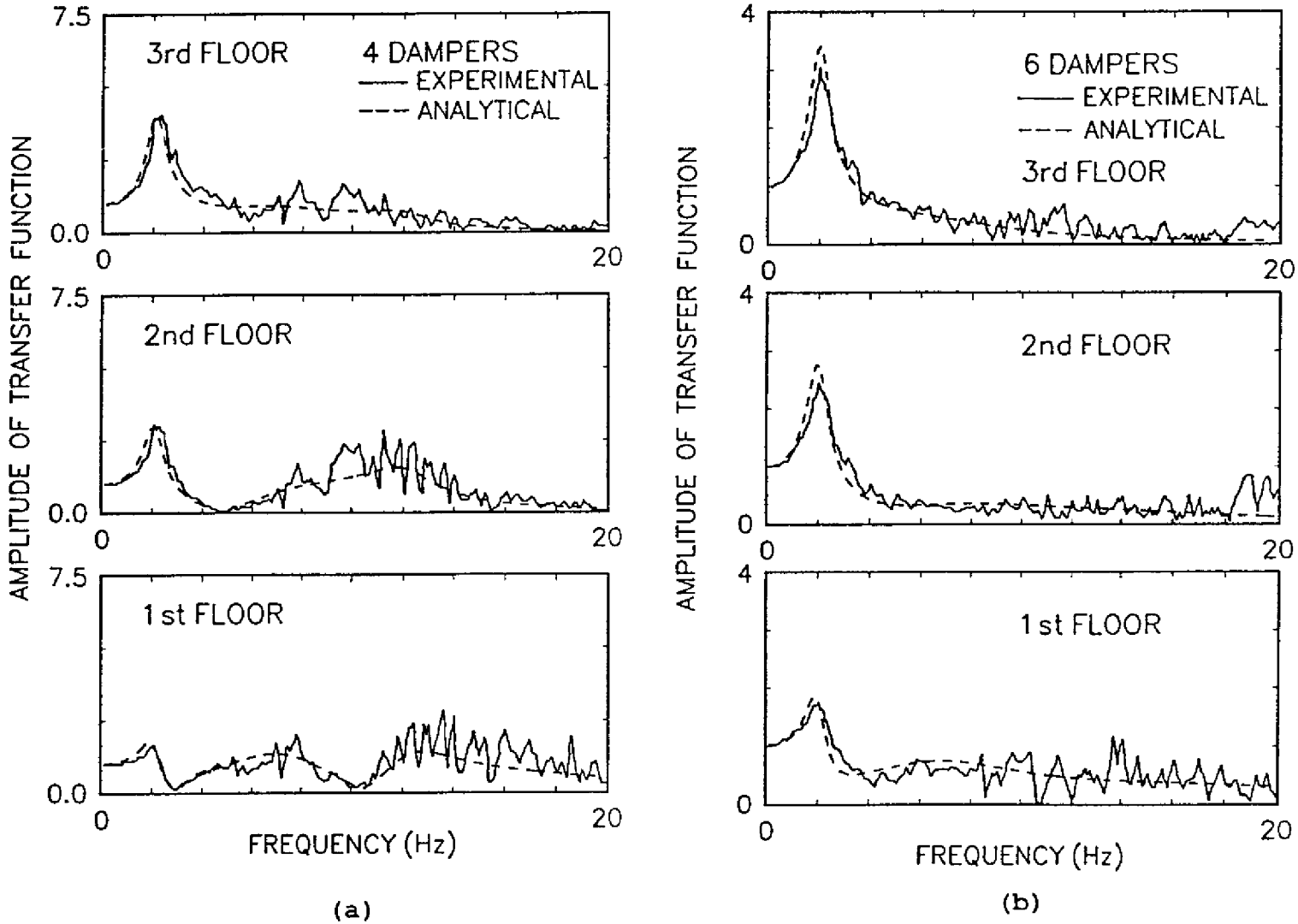

FIGURE 4-3 Comparison of Analytical and Experimental Amplitudes of Transfer Functions of 3-story Structure with (a) Four Dampers and (b) Six Dampers

very good. This indicates that the calculated properties are indeed very good estimates of the true properties.

In Figure 4-3(b), it is particularly interesting to note that the amplitude of the transfer functions of the 3-story structure with dampers at every story contains a single peak close to the fundamental frequency. The higher modes are completely suppressed. Therefore, the structure may be analyzed as a single degree of freedom system.

Finally, Figure 4-4 compares the amplitudes of transfer functions of the 3-story structure with two fluid dampers installed at the first story as calculated using the general Maxwell model of Equation 2-13 and the simple viscous model of Equation 2-19. The latter case is produced in Equation 4-31 by setting $\lambda = 0$. The difference between the two models consists of a minor shift in the frequency position of the higher mode peaks.

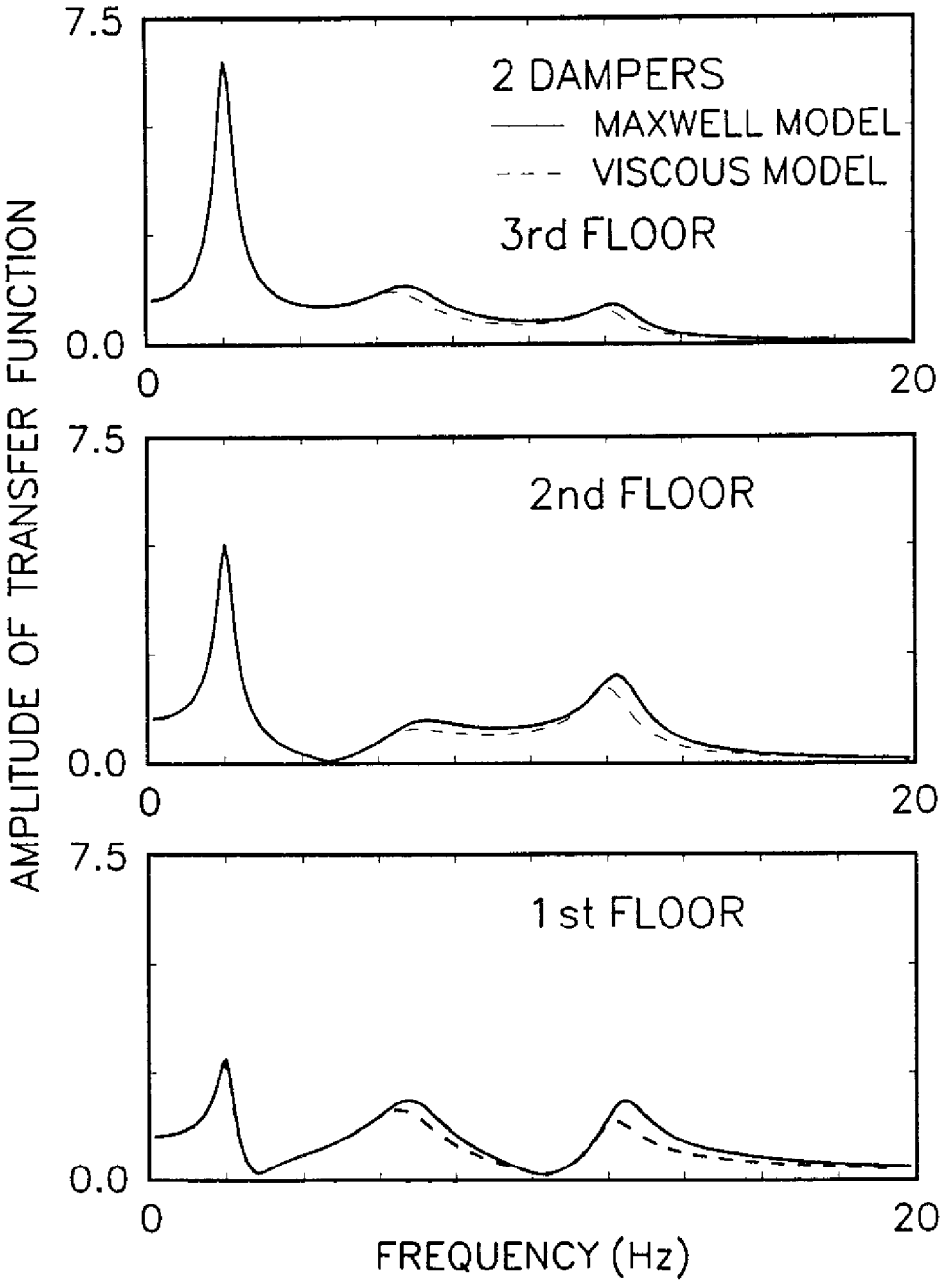

FIGURE 4-4 Comparisons of Amplitudes of Transfer Functions of 3-story Structure with Two Dampers Based on Analytical Maxwell Model and Analytical Viscous Model

SECTION 5
EARTHQUAKE SIMULATOR TEST RESULTS

5.1 One-story Structure

The experimental results for the unstiffened and stiffened structure are summarized in Tables 5-I and 5-II, respectively. For each test, the peak values of the table motion in the horizontal direction are given. The displacement and acceleration were directly measured whereas the velocity was determined by numerical differentiation of the displacement record. The peak drift is given as a percentage of the story height which was 32 inches (813 mm). In addition, the peak drift has been determined based upon the horizontal component of the damper displacement. There is a quantitative difference between the two values of the peak drift which has been attributed to slipping at the bolted connections between the structural frame and the lateral bracing. The peak base shear was calculated from the known masses and recorded accelerations and is given as a fraction of the total weight (6446 lb or 28743 N) of the structure.

Results in graphical form for all tests are presented in Appendix A. The graphs present recorded loops of base shear force over weight ratio versus the first story drift. Furthermore, for each test, the graphs of Appendix A present the contributions to the base shear from the fluid dampers and the columns. It is evident in these graphs that the contribution from the fluid dampers to the base shear - drift loops is purely of a viscous nature and accordingly the dampers display no stiffness. This confirms that the additional column axial load due to the damper forces occurs out-of-phase with the peak drift so that column compression failure is not a concern (see also Section 1 and Figure 1-7).

TABLE 5-I Summary of Experimental Results for Unstiffened One-story Structure
(1 in. = 25.4 mm)

TEST	EXCITATION	DMP	SYSTEM PARAMETERS		PEAK TABLE MOTION (Horiz)			$\frac{\text{PEAK BASE SHEAR}}{\text{WEIGHT}}$	$\frac{\text{PEAK DRIFT}}{\text{HEIGHT}}$ (%)	$\frac{\text{PEAK DRIFT}^{\star}}{\text{HEIGHT}}$ (%)
			f (Hz)	ξ (%)	DISPL. (in)	VELOC. (in/sec)	ACCEL. (g's)			
1	El Centro 10%	0	2.00 [1]	0.55 [2]	0.093	0.656	0.038	0.085	0.623	---
2	El Centro 20%	0	2.00 [1]	0.55 [2]	0.188	1.259	0.071	0.160	1.205	---
3	El Centro 33.3%	0	2.00 [1]	0.55 [2]	0.310	2.022	0.107	0.228	1.842	---
4	Taft 33.3%	0	2.00 [1]	0.55 [2]	0.185	0.838	0.044	0.091	0.688	---
5	Taft 66.7%	0	2.00 [1]	0.55 [2]	0.374	1.666	0.097	0.153	1.134	---
6	Taft 100%	0	2.00 [1]	0.55 [2]	0.562	2.475	0.144	0.224	1.740	---
7	Taft 100%	2	2.04	28.4	0.563	2.491	0.151	0.129	0.724	0.689
8	Taft 100% (H&V)	2	2.04	28.4	0.566	2.491	0.148	0.130	0.775	0.702
9	El Centro 33.3%	2	2.04	28.4	0.309	2.125	0.106	0.087	0.500	0.469
10	El Centro 66.7%	2	2.04	28.4	0.618	4.009	0.197	0.168	1.071	0.997
11	El Centro 100%	2	2.04	28.4	0.947	6.275	0.310	0.259	1.693	1.576
12	Miyagiken 100%	2	2.04	28.4	0.479	2.403	0.155	0.115	0.636	0.754
13	Miyagiken 200%	2	2.04	28.4	0.961	4.622	0.308	0.234	1.459	1.688
14	Hachinohe 50%	2	2.04	28.4	0.644	2.625	0.116	0.122	0.806	0.930
15	Hachinohe 100%	2	2.04	28.4	1.291	5.172	0.215	0.247	1.645	1.808

DMP = Number of Dampers
f = Undamped Frequency
* = Measured from Component of Damper Displacement
H&V = Horizontal and Vertical Components
Note 1: 2.00 to 1.94 Hz Depending on the Amplitude of Motion
Note 2: 0.55 to 2.2% Depending on the Amplitude of Motion

TABLE 5-I Continued

TEST	EXCITATION	DMP	SYSTEM PARAMETERS		PEAK TABLE MOTION (Horiz)			PEAK BASE SHEAR / WEIGHT	PEAK DRIFT / HEIGHT (%)	PEAK DRIFT * / HEIGHT (%)
			f (Hz)	ξ (%)	DISPL. (in)	VELOC. (in/sec)	ACCEL. (g's)			
16	El Centro 100%	4	2.10	57.7	0.947	6.244	0.298	0.301	1.031	1.002
17	Taft 100%	4	2.10	57.7	0.562	2.491	0.145	0.115	0.504	0.467
18	Miyagiken 200%	4	2.10	57.7	0.962	4.613	0.305	0.200	0.870	0.815
19	Hachinohe 100%	4	2.10	57.7	1.290	5.272	0.216	0.214	1.114	1.026
20	Taft 200%	4	2.10	57.7	1.132	4.900	0.301	0.226	1.067	0.966
21	Taft 300%	4	2.10	57.7	1.700	7.428	0.476	0.342	1.667	1.514
22	El Centro 150%	4	2.10	57.7	1.418	9.509	0.487	0.456	1.563	1.402
23	Miyagiken 320%	4	2.10	57.7	1.635	7.822	0.536	0.338	1.564	1.307
24	Hachinohe 150%	4	2.10	57.7	1.938	7.959	0.319	0.321	1.742	1.490
25	Pacoima Dam 50%	4	2.10	57.7	0.598	5.556	0.452	0.278	1.155	0.993
26	Pacoima Dam 75%	4	2.10	57.7	0.897	8.409	0.658	0.412	1.755	1.626

DMP = Number of Dampers
f = Undamped Frequency
* = Measured From Component of Damper Displacement

TABLE 5-II Summary of Experimental Results for Stiffened One-story Structure
(1 in. = 25.4 mm)

TEST	EXCITATION	DMP	SYSTEM PARAMETERS		PEAK TABLE MOTION (Horiz)			PEAK BASE SHEAR / WEIGHT	PEAK DRIFT / HEIGHT (%)	PEAK DRIFT * / HEIGHT (%)
			f (Hz)	ξ (%)	DISPL. (in)	VELOC. (in/sec)	ACCEL. (g's)			
50	El Centro 33.3%	0	3.13 [1]	2.0 [1]	0.318	2.138	0.110	0.300	0.970	---
51	Taft 100%	0	2.99 [1]	2.9 [1]	0.561	2.484	0.144	0.431	1.479	---
52	El Centro 33.3%	0 [2]	3.15 [1]	4.8 [1]	0.318	2.134	0.112	0.276	0.853	---
53	Taft 100%	0 [2]	3.17 [1]	5.1 [1]	0.561	2.516	0.147	0.307	0.944	---
54	El Centro 33.3%	2	3.27	19.3	0.318	2.094	0.110	0.203	0.635	0.547
55	El Centro 66.7%	2	3.27	19.3	0.632	4.222	0.199	0.393	1.230	1.101
56	Taft 100%	2	3.27	19.3	0.563	2.494	0.145	0.226	0.667	0.594
57	Taft 200%	2	3.27	19.3	1.129	4.912	0.300	0.424	1.362	1.228
58	Hachinohe 100%	2	3.27	19.3	1.289	5.234	0.215	0.263	0.858	0.725
59	Hachinohe 150%	2	3.27	19.3	1.935	7.900	0.324	0.383	1.262	1.118
60	El Centro 33.3%	4	3.35	37.4	0.320	2.084	0.114	0.173	0.441	0.372
61	El Centro 66.7%	4	3.35	37.4	0.632	4.178	0.201	0.335	0.874	0.779
62	El Centro 100%	4	3.35	37.4	0.947	6.281	0.304	0.485	1.305	1.186
63	Taft 100%	4	3.35	37.4	0.561	2.556	0.148	0.180	0.437	0.410
64	Taft 200%	4	3.35	37.4	1.129	4.972	0.304	0.342	0.920	0.819
65	Taft 300%	4	3.35	37.4	1.695	7.425	0.487	0.504	1.405	1.247
66	Hachinohe 150%	4	3.35	37.4	1.934	7.878	0.326	0.330	0.979	0.862

DMP = Number of Dampers
f = Undamped Frequency
* = Measured from Component of Damper Displacement
Note 1: Measured From Hysteresis Loop under Seismic Excitation
Note 2: Wire Rope Cables Attached to Increase Energy Dissipation

5.2 Three-story Structure

The experimental results for the three-story tests are given in Table 5-III. For each test, the peak values of the table motion in the horizontal direction are given. The peak drift is given as a percentage of the story height which was 32 inches (813 mm) for the first story and 30 inches (762 mm) for the second and third story. In addition, the peak drift of the first story has been determined based upon the horizontal component of the damper displacement. The quantitative difference between the two values is again a result of slipping at the bolted connections between the structural frame and the lateral bracing. The peak acceleration at each floor is given and the peak shear force at each story is given as a fraction of the total weight (6332 lb or 28235 N) of the structure.

Plots of recorded story shear force over total weight ratio versus story drift for all tests are presented in Appendix B.

5.3 Effectiveness of Dampers

A number of observations related to the effectiveness of fluid dampers are made from the results of Tables 5-I through 5-III and from Appendices A and B.

5.3.1 Reduction of Response

A comparison of responses between the one-story structure without and with fluid dampers reveals ratios of peak story drift in the damped structure to peak story drift in the undamped moment-resisting frame structure, RD, in the range of 0.3 to 0.7 and ratios of peak base shear force in the damped structure to peak base shear force in the undamped structure, RBS, in the range of 0.4 to 0.7. These significant reductions in response are a result of the increased ability to dissipate energy and are not a result of changes in stiffness.

TABLE 5-III Summary of Experimental Results for 3-story Structure (1 in. = 25.4 mm)

TEST	EXCITATION	DMP	SYSTEM PARAMETERS		PEAK TABLE MOTION (Horiz)			PEAK ACCELERATION (g's)		
			f (Hz)	ξ (%)	DISPL. (in)	VELOC. (in/sec)	ACCEL. (g's)	1st Floor	2nd Floor	3rd Floor
27	El Centro 33.3%	0	2.00 [1]	1.74 [1]	0.317	2.138	0.109	0.275	0.308	0.417
28	El Centro 50%	0	2.00 [1]	1.74 [1]	0.477	3.169	0.157	0.389	0.410	0.585
29	Taft 100%	0	2.00 [1]	1.74 [1]	0.562	2.472	0.146	0.424	0.403	0.555
30	El Centro 50%	6	2.03	19.4	0.475	3.134	0.152	0.127	0.152	0.205
31	El Centro 100%	6	2.03	19.4	0.949	6.322	0.312	0.205	0.286	0.368
32	El Centro 150%	6	2.03	19.4	1.419	9.447	0.485	0.340	0.402	0.534
33	Taft 100%	6	2.03	19.4	0.562	2.516	0.145	0.140	0.136	0.178
34	Taft 200%	6	2.03	19.4	1.131	4.994	0.300	0.253	0.264	0.348
35	Taft 300%	6	2.03	19.4	1.700	7.416	0.465	0.362	0.379	0.513
36	Hachinohe 100%	6	2.03	19.4	1.290	5.325	0.215	0.248	0.276	0.334
37	Miyagiken 200%	6	2.03	19.4	1.036	5.003	0.326	0.247	0.271	0.342
38	Pacoima Dam 50%	6	2.03	19.4	0.596	5.538	0.455	0.282	0.308	0.376
39	Pacoima Dam 50% (H&V)	6	2.03	19.4	0.555	5.244	0.419	0.273	0.314	0.377
40	El Centro 100% (H&V)	6	2.03	19.4	0.938	6.147	0.298	0.239	0.293	0.390
41	Taft 200% (H&V)	6	2.03	19.4	1.133	5.013	0.316	0.243	0.283	0.352
42	El Centro 50%	2	2.03	9.9	0.471	3.116	0.156	0.220	0.286	0.301
43	El Centro 75%	2	2.03	9.9	0.710	4.663	0.225	0.316	0.391	0.427
44	Taft 100%	2	2.03	9.9	0.563	2.541	0.147	0.172	0.218	0.271
45	Taft 200%	2	2.03	9.9	1.129	4.975	0.298	0.345	0.426	0.545
46	El Centro 50%	4	2.11	17.7	0.474	3.209	0.156	0.170	0.221	0.282
47	El Centro 100%	4	2.11	17.7	0.948	6.447	0.304	0.346	0.476	0.591
48	Taft 100%	4	2.11	17.7	0.561	2.494	0.145	0.161	0.208	0.246
49	Taft 200%	4	2.11	17.7	1.130	4.947	0.299	0.324	0.383	0.464

TABLE 5-III Continued

TEST	EXCITATION	DMP	SYSTEM PARAMETERS		PEAK SHEAR FORCE / WEIGHT			PEAK DRIFT / HEIGHT (%)			PEAK DRIFT * / HEIGHT (%)
			f (Hz)	ξ (%)	1st Story	2nd Story	3rd Story	1st Story	2nd Story	3rd Story	1st Story
27	El Centro 33.3%	0	2.00 [1]	1.74 [1]	0.220	0.199	0.139	0.976	1.069	0.769	---
28	El Centro 50%	0	2.00 [1]	1.74 [1]	0.295	0.272	0.195	1.386	1.498	1.073	---
29	Taft 100%	0	2.00 [1]	1.74 [1]	0.255	0.200	0.185	1.161	1.077	0.911	---
30	El Centro 50%	6	2.03	19.4	0.138	0.108	0.068	0.489	0.510	0 281	0.471
31	El Centro 100%	6	2.03	19.4	0.261	0.208	0.123	0 993	0.998	0.600	0.943
32	El Centro 150%	6	2.03	19.4	0.368	0.298	0.178	1.436	1.492	0.852	1.382
33	Taft 100%	6	2.03	19.4	0.120	0.104	0.059	0.425	0.463	0.253	0.399
34	Taft 200%	6	2.03	19.4	0.235	0.198	0.116	0.900	0.921	0.546	0.830
35	Taft 300%	6	2.03	19.4	0.343	0.288	0.171	1.407	1.369	0.819	1.270
36	Hachinohe 100%	6	2.03	19.4	0.256	0.201	0.111	1.036	0.963	0.575	0.957
37	Miyagiken 200%	6	2.03	19.4	0.254	0.202	0.114	0.947	0.963	0.610	0.890
38	Pacoima Dam 50%	6	2.03	19.4	0.275	0.224	0.125	1.106	1.017	0.629	1.003
39	Pacoima Dam 50% (H&V)	6	2.03	19.4	0.260	0.214	0.126	1.021	0.956	0.652	0.951
40	El Centro 100% (H&V)	6	2.03	19.4	0.260	0.202	0.130	0.998	1.029	0.588	0.941
41	Taft 200% (H&V)	6	2.03	19.4	0.236	0.195	0.117	0.929	0.931	0.531	0.829
42	El Centro 50%	2	2.03	9.9	0.196	0.159	0.100	0.806	0.865	0.548	0.750
43	El Centro 75%	2	2.03	9.9	0.282	0.233	0.142	1.210	1.292	0.785	1.124
44	Taft 100%	2	2.03	9.9	0.150	0.148	0.090	0.626	0.696	0.500	0.574
45	Taft 200%	2	2.03	9.9	0.296	0.279	0.182	1.247	1.431	0.983	1.181
46	El Centro 50%	4	2.11	17.7	0.159	0.132	0.094	0.540	0.660	0.465	0.520
47	El Centro 100%	4	2.11	17.7	0.314	0.256	0.197	1.142	1.279	0.933	1.081
48	Taft 100%	4	2.11	17.7	0.118	0.130	0.082	0.411	0.638	0.465	0.388
49	Taft 200%	4	2.11	17.7	0.253	0.249	0.155	0.949	1.208	0.829	0.887

DMP = Number of Dampers, f = Undamped Frequency, * = Measured from Component of Damper Displacement
Note 1: For Small Amplitude of Vibration, H&V = Horizontal and Vertical Components

The corresponding ratios of story drift and story shear force in the 3-story structure are lower and typically in the range of 0.3 to 0.5. The lower values of these ratios in the 3-story structure in comparison to the one-story structure is merely the result of lower damping in the bare frame of the 3-story structure. For this, the reader should recall the results of Tables 4-I and 4-II.

A comparison of responses of the 3-story structure without and with fluid dampers is presented in Figure 5-1. Clearly, the addition of fluid dampers resulted in overall significant reduction of accelerations, story shear forces and interstory drifts.

A different comparison of responses is presented in Figure 5-2, which presents profiles of response of the 3-story structure without and with dampers at two different levels of the same earthquake. Evidently, the responses of the two systems are approximately the same for two significantly different levels of the same earthquake. It may be stated that, for this particular earthquake, the addition of fluid dampers has increased the earthquake resistance of the moment resisting bare frame by three-fold. Of course, this is not generally the case. An inspection of the acceleration spectra in Figures 3-10 to 3-14, shows that the reduction achieved by increasing damping from 5 to 20% of critical depends on the period of the structure and the content in frequency of the excitation.

It is interesting to note in Figure 5-2 that the base shear force in the damped structure is larger than that of the undamped structure despite the overall lower accelerations. This is explained by considering the differences in the contribution of the higher modes of the two systems. In the undamped structure, the peak values of floor accelerations occur at different times as a result of contributions from the higher modes. In the damped structure, higher modes are almost completely suppressed and the peak values of floor accelerations occur at almost identical times.

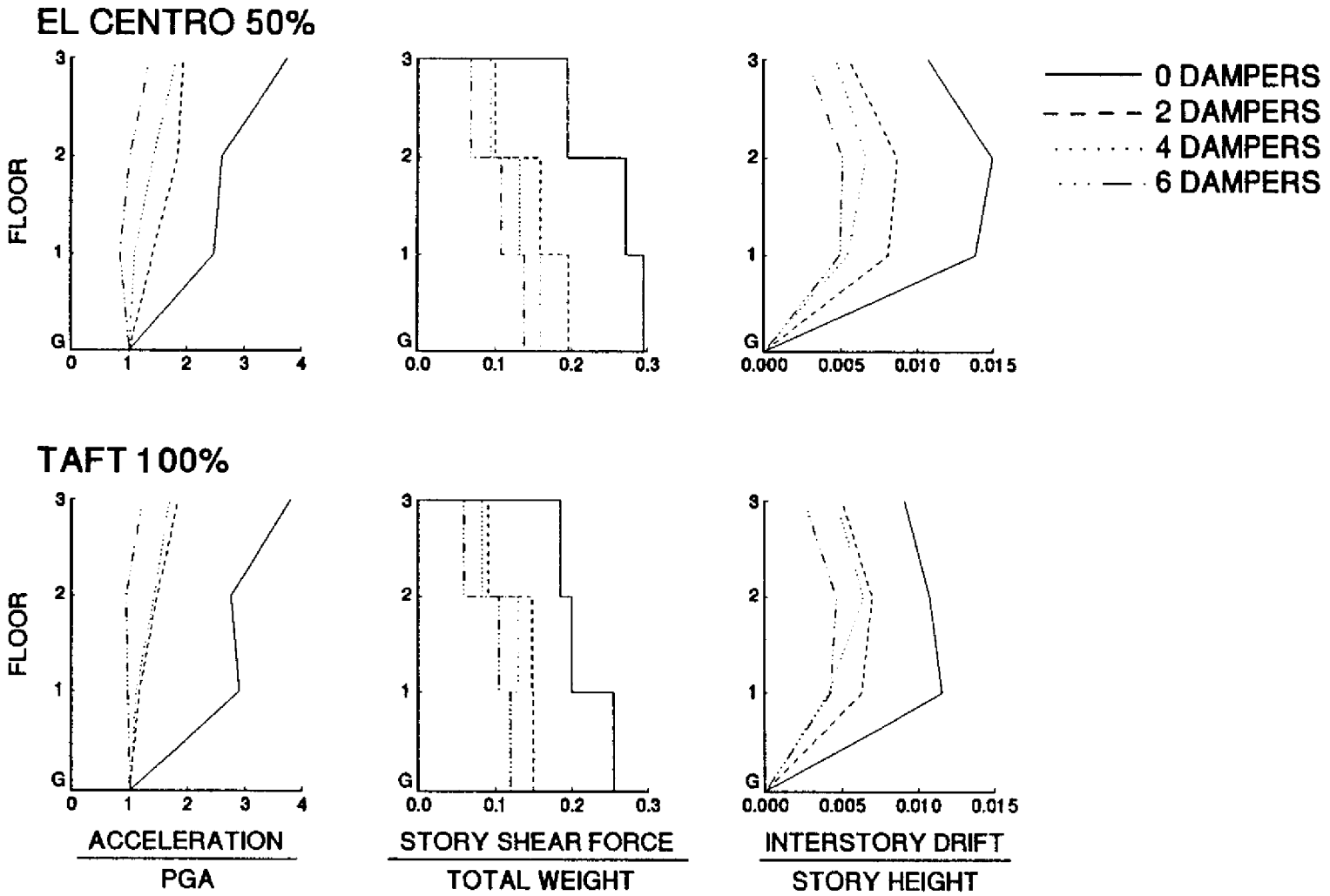

FIGURE 5-1 **Acceleration, Story Shear and Interstory Drift Profiles of 3-story Structure**

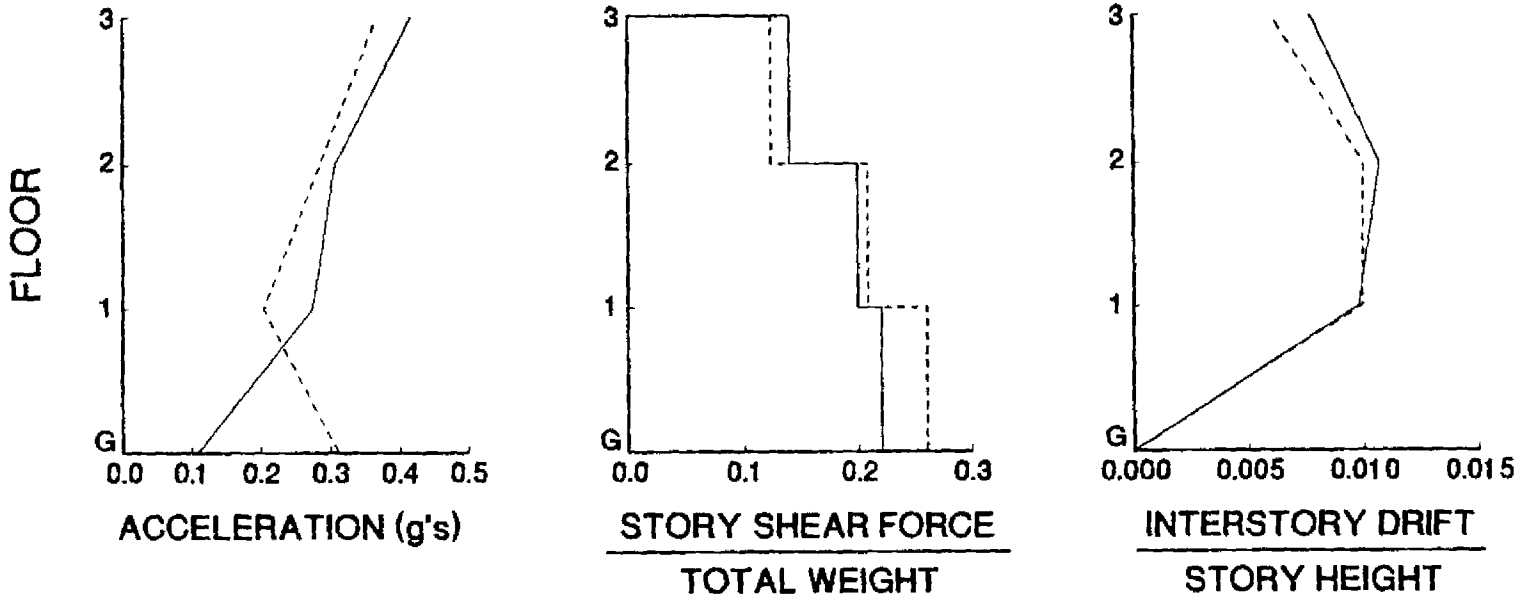

FIGURE 5-2 Comparison of Response Profiles for Two Different Levels of the Same Earthquake

5.3.2 Effect of Vertical Ground Motion

An observation to be made from Tables 5-I and 5-III is the effect that the vertical ground motion has on the response of the damped structure. The response, in terms of story drifts and shear forces, is affected. The effect is either a minor mixed increase and decrease of various response quantities or a minor net reduction of response. In general, this effect appears to be negligible.

5.3.3 Energy Dissipation

The effect of fluid dampers on the behavior of a structural system to which they are attached is vividly illustrated in graphs of the time history of the energy dissipated by various mechanisms in the structure. Figure 5-3 shows energy time histories for the one-story structure subjected to the Taft 100% motion. The energies were calculated from the equation of motion (Equation 4-1) after multiplication by du and integration over the time interval 0 to t. The result is (see also Section 1)

$$E = E_k + E_s + E_h + E_d \tag{5-1}$$

where

$$E = \int_0^t m(\ddot{u} + \ddot{u}_g)\, du_g \tag{5-2}$$

is the absolute energy input,

$$E_k = \frac{1}{2} m(\dot{u} + \dot{u}_g)^2 \tag{5-3}$$

is the kinetic energy,

$$E_s = \frac{1}{2} k u^2 \tag{5-4}$$

is the recoverable strain energy,

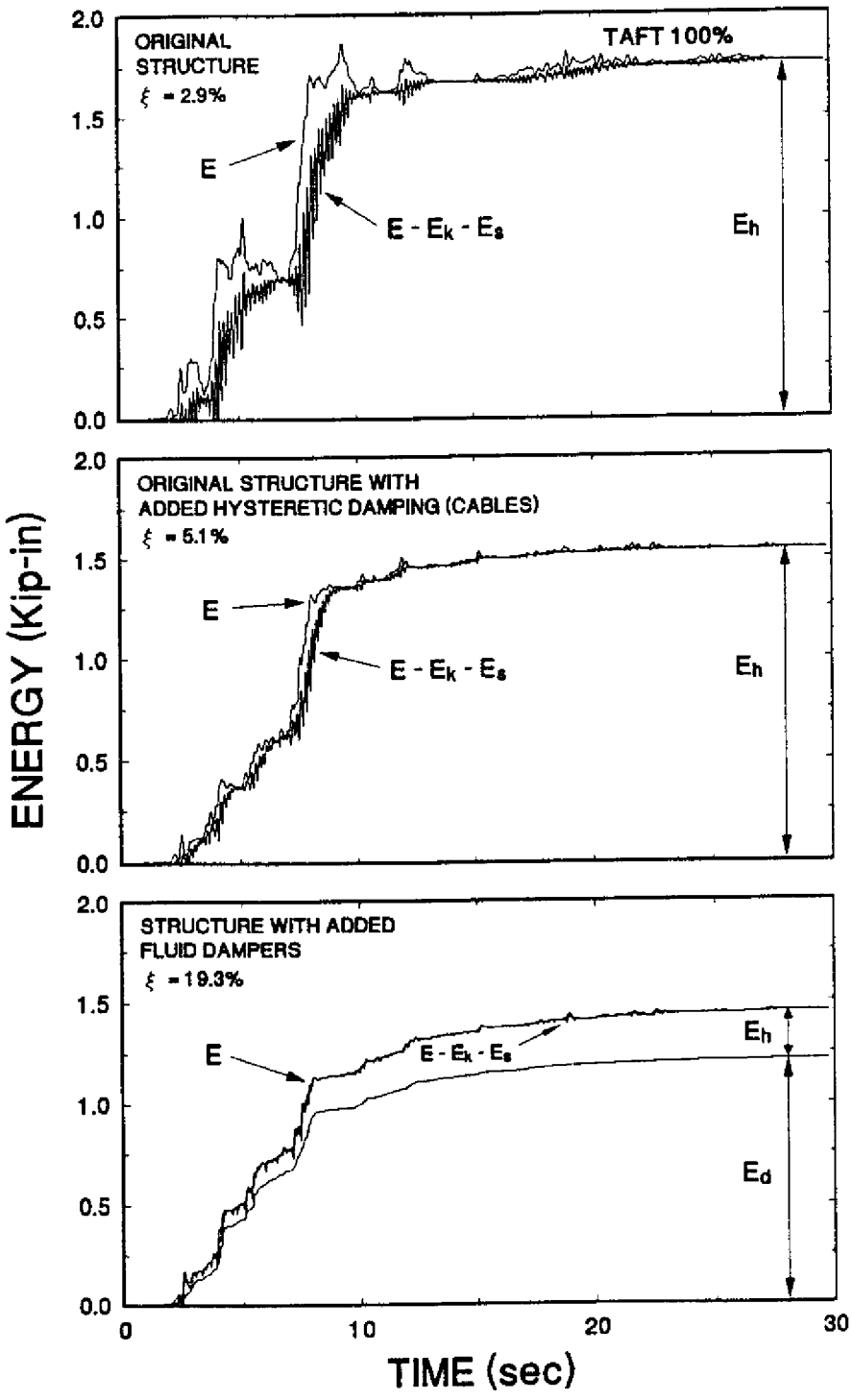

FIGURE 5-3 Energy Time Histories in One-story Stiffened Structure Subjected to Taft 100% Motion (1 Kip = 4.46 KN, 1 in. = 25.4 mm)

$$E_d = \int_0^t \eta P_d \, du \qquad (5\text{-}5)$$

is the energy dissipated by the fluid dampers, and E_h is the energy dissipated by other mechanisms in the structural frame (by viscous and hysteretic actions).

Figure 5-3 demonstrates a reduction of the absolute input energy with the addition of fluid dampers. Furthermore, the kinetic and strain energies are reduced. This demonstrates the reduction of structural deformation. However, the most beneficial effect is the significant reduction of the energy dissipated in the structural frame in exchange for energy dissipation by the fluid dampers.

5.3.4 Effect of Position of Fluid Dampers

The 3-story structure was tested in two different configurations. In the first, fluid dampers were placed at all stories (case of 6 dampers). In the second, fluid dampers were placed only at the first story (cases of 2 and 4 dampers). The primary effect of the difference in configuration was that damping in the fundamental mode varied from 9.9% (2 dampers) to 17.7% (4 dampers) to 19.4% of critical (6 dampers). The secondary effect was substantial differences in the higher mode characteristics of the three systems (see Table 4-II).

In terms of response of the three systems, Figure 5-1 provides a comparison of the systems for two earthquakes. Evidently, the concentration of the fluid dampers at one level did not have any adverse effect. The observed differences in the response of the three systems is just a result of a difference in the damping of the fundamental mode.

It should be noted that, in general, this behavior can be achieved by placing fluid dampers at those stories where the largest interstory velocity is expected. For response primarily in the first mode, this occurs at the story with maximum drift in the mode shape.

In effect, increases in damping may be achieved either by distribution of several fluid dampers over the height of the structure, or by strategically placing larger dampers at few locations. The only drawback of such an approach is the development of larger forces at a few joints and the reduction in damper redundancy.

5.4 Comparison with Other Energy Absorbing Systems

Direct comparison of responses of different structural systems to earthquakes is very difficult. Typically, a relatively small difference in the period of the structure may lead to dramatic changes in the response when the spectrum of the excitation exhibits significant changes in the range of periods containing the respective fundamental periods.

However, comparisons of indirect response quantities, such as ratios of a particular response quantity in the damped structure to the same quantity in the undamped structure, may provide some limited insight into the behavior of various energy absorbing systems.

For this, we utilize recorded ratios of peak drift responses, RD, and peak base shear force, RBS. Table 5-IV provides a comparison of these quantities for various energy absorbing systems.

The results in Table 5-IV demonstrate that all systems may produce reductions in drift which are comparable. Furthermore, fluid dampers produce reductions in base shear force which are not

TABLE 5-IV Comparison of Drift (RD) and Base Shear Force (RBS) Response Ratios of Various Energy Absorbing Systems

SYSTEM	RD	RBS	REFERENCE
Viscoelastic Dampers	0.5 - 0.9	~ 1	Aiken, 1990
Friction Dampers	0.5 - 0.9	~ 1	Aiken, 1990
Yielding Steel Dampers	0.3 - 0.7	0.6 - 1.25	Whittaker, 1989
Fluid Dampers	0.3 - 0.7	0.4 - 0.7	This Study

realized in the other energy absorbing systems. The reason for this behavior is the effectively viscous nature of fluid dampers. As stated earlier, this behavior has a further advantage in that the additional column axial forces are out-of-phase with the peak drift (see Figure 1-7).

In summary, the addition of fluid dampers significantly reduced both the peak base shear and peak drift in all tests performed. The simultaneous reduction of both of these response quantities is desirable in that the shear forces transmitted to the supporting columns are reduced and, at the same time, the non-structural elements are subjected to lower levels of relative displacement. With currently available seismic protection techniques, other than seismic isolation, it is often difficult to simultaneously reduce both of these response quantities.

5.5 Comparison with Active Control

Active control systems are based on the development of external forces (e.g., developed by actuators or actively moving masses) and have been extensively studied. Soong (1990) demonstrated that the effect of the active control is to primarily modify the structural properties of stiffness and damping. In fact, successful experimental studies with an active tendon system (Chung 1989 and Soong 1990) demonstrated that the primary effect of active control was to increase damping of the tested system with only minor or insignificant modification of stiffness.

In this respect, the achievements of active control may be reproduced and exceeded by fluid viscous dampers with the following additional advantages:

a) Low Cost. Low cost is primarily achieved by utilizing the motion of the structure itself to generate the required damping forces rather than using other means which are external to the structural system (e.g., actuators).

b) Reliability. Fluid dampers have demonstrated good performance over the last twenty years in military applications.

c) Power Requirements. Fluid dampers do not have external power requirements.

d) Longevity. Fluid dampers have been subjected to many years of continuous use in the harsh environment of military applications.

In Table 5-V, the experimental results obtained with the 3-story model structure are compared against the results obtained with the same structure and an active control system (Chung 1989 and Soong 1990). This table compares the recorded response of the structure subjected to the 1940 El Centro, component S00E excitation when uncontrolled and when controlled by either an active tendon system or by fluid dampers. It is evident in this table that the effect of the active tendon system is to only modify damping, an effect which can be reliably produced by fluid dampers. Actually, the level of damping achieved by the fluid dampers is such that, for this particular structure and excitation, the fluid dampers exhibit a clearly superior performance to that of active control.

TABLE 5-V Comparison of Response of Tested 3-Story Model Structure

CONTROL METHOD	SYSTEM PARAMETERS		EXCITATION	FLOOR OR STORY	PEAK FLOOR ACCEL. (g's)	*PEAK INTERSTORY DRIFT / HEIGHT* (%)
	f (Hz)	ξ (%)				
Uncontrolled	2.24 6.83 11.53	1.62 0.39 0.36	El Centro S00E PGA=0.085g	3 2 1	0.322 0.221 0.158	0.596 0.874 0.667
Active Tendon System	2.28 6.94 11.56	12.77 12.27 5.45	El Centro S00E PGA=0.085g	3 2 1	0.200 0.138 0.139	0.405 0.592 0.392
Uncontrolled	2.00 6.60 12.20	1.74 0.76 0.34	El Centro S00E PGA=0.157g	3 2 1	0.585 0.410 0.389	1.073 1.498 1.386
Six Fluid Dampers Placed at all Stories	2.03 7.64 16.99	19.40 44.70 38.04	El Centro S00E PGA=0.152g	3 2 1	0.205 0.152 0.127	0.281 0.510 0.489
Four Fluid Dampers Placed at First Story	2.11 7.52 12.16	17.70 31.85 11.33	El Centro S00E PGA=0.156g	3 2 1	0.282 0.221 0.170	0.465 0.660 0.540